

Cardiac and Skeletal Muscle Insulin Resistance in Patients with Coronary Heart Disease

A Study with Positron Emission Tomography

Giovanni Paternostro,* Paolo G. Camici,* Adriaan A. Lammerstma,* Norma Marinho,* Ragavendra R. Baliga,* Jaspal S. Kooner,* George K. Radda,† and Ele Ferrannini‡

*Medical Research Council Clinical Sciences Center and the Royal Postgraduate Medical School, Hammersmith Hospital, London, United Kingdom; †Department of Biochemistry, University of Oxford, Oxford, United Kingdom; and ‡the Metabolism Unit of the Consiglio Nazionale delle Ricerche, Institute of Clinical Physiology, Pisa, Italy

Abstract

Patients with coronary artery disease or heart failure have been shown to be insulin resistant. Whether in these patients heart muscle participates in the insulin resistance, and whether reduced blood flow is a mechanism for such resistance is not known. We measured heart and skeletal muscle blood flow and glucose uptake during euglycemic hyperinsulinemia (insulin clamp) in 15 male patients with angiographically proven coronary artery disease and chronic regional wall motion abnormalities. Six age- and weight-matched healthy subjects served as controls. Regional glucose uptake was measured by positron emission tomography using [¹⁸F]2-fluoro-2-deoxy-D-glucose (FDG), blood flow was measured by the H₂¹⁵O method. Myocardial glucose utilization was measured in regions with normal perfusion and wall motion as assessed by radionuclide ventriculography. Whole-body glucose uptake was $37 \pm 4 \mu\text{mol} \cdot \text{min}^{-1} \cdot \text{kg}^{-1}$ in controls and $14 \pm 2 \mu\text{mol} \cdot \text{min}^{-1} \cdot \text{kg}^{-1}$ in patients ($P = 0.001$). Myocardial blood flow (1.09 ± 0.06 vs. $0.97 \pm 0.04 \text{ ml} \cdot \text{min}^{-1} \cdot \text{g}^{-1}$, controls vs. patients) and skeletal muscle (arm) blood flow (0.046 ± 0.012 vs. $0.043 \pm 0.006 \text{ ml} \cdot \text{min}^{-1} \cdot \text{g}^{-1}$) were similar in the two groups ($P = \text{NS}$ for both). In contrast, in patients both myocardial (0.38 ± 0.03 vs. $0.70 \pm 0.03 \mu\text{mol} \cdot \text{min}^{-1} \cdot \text{g}^{-1}$, $P = 0.0005$) and muscle glucose uptake (0.026 ± 0.004 vs. $0.056 \pm 0.006 \mu\text{mol} \cdot \text{min}^{-1} \cdot \text{g}^{-1}$, $P = 0.005$) were markedly reduced in comparison with controls. In the whole dataset, a direct relationship existed between insulin-stimulated glucose uptake in heart and skeletal muscle.

Patients with a history of myocardial infarction and a low ejection fraction are insulin resistant. This insulin resistance affects both the myocardium and skeletal muscle and is independent of blood flow. (*J. Clin. Invest.* 1996. 98:2094–2099.) Key words: insulin resistance • coronary heart disease • skeletal muscle • myocardial muscle

Introduction

Insulin resistance is commonly defined as a decreased response of glucose uptake to the stimulatory effect of insulin (1). Glucose is an especially important substrate for the heart (2), and influences both normal cardiac function (3) and the response of the heart to ischemia (4). Insulin promotes glucose uptake and decreases the utilization of free fatty acids by the human heart (5, 6). A decrease in glycolysis has been shown in various animal models of heart failure (7), and, more recently, heart failure has also been linked with insulin resistance (8). In ischemic myocardium, on the other hand, glycolysis is accelerated through an activation of the insulin-sensitive glucose transporter (GLUT-4), a phenomenon thought to have a cardioprotective role (9).

In patients with insulin-dependent diabetes (IDDM), peripheral (skeletal muscle) insulin resistance is not accompanied by a defect in cardiac [¹⁸F]2-fluoro-2-deoxy-D-glucose (FDG)¹ uptake, as measured by positron-emitting tomography (PET) (10, 11). In contrast, reduced cardiac FDG uptake has been reported by Voipio Pulkki et al. in patients with non-insulin dependent diabetes mellitus (NIDDM) (12) in whom, however, there was no evidence of peripheral (skeletal muscle) insulin resistance, a prevalent abnormality in this form of diabetes (1). On the other hand, in young subjects with mild hypertension and no cardiac hypertrophy, Nuutila et al. (13) could show skeletal but not cardiac insulin resistance. Thus, the involvement of the heart in conditions of systemic insulin resistance remains uncertain.

In the present work, glucose uptake and blood flow in both cardiac and skeletal muscle were quantitated simultaneously. The methodology involved the combination of the insulin clamp technique with PET measurements of glucose uptake (¹⁸FDG) and blood flow (H₂¹⁵O). Euglycemic hyperinsulinemia measures whole-body insulin resistance and enhances the FDG signal during PET (14). The model chosen was the non-infarcted myocardium of patients who have suffered from an acute myocardial infarction.

Methods

Patients. The patient population consisted of 15 normotensive, non-diabetic men (aged 54 ± 2 years, range 34–62) with coronary artery disease. All patients had suffered a previous myocardial infarction at least 6 mo before the study. All patients had at least one ventricular

Address correspondence to Dr. Giovanni Paternostro, MRC Clinical Sciences Center, Hammersmith Hospital, Du Cane Road, London W12 0NN. Phone: 44-181-3833162; FAX: 44-181-3832029.

Received for publication 11 June 1996 and accepted in revised form 28 August 1996.

J. Clin. Invest.

© The American Society for Clinical Investigation, Inc.

0021-9738/96/11/2094/06 \$2.00

Volume 98, Number 9, November 1996, 2094–2099

1. **Abbreviations used in this paper:** FDG, [¹⁸F]2-fluoro-2-deoxy-D-glucose; FWHM, full width at half maximum; PET, positron-emitting tomography; ROI, regions of interest; SGU, skeletal muscle glucose uptake.

region with normal motility—as assessed by radionuclide ventriculography—and with normal blood flow (i.e., within 1 SD of the mean myocardial blood flow in our database of normal subjects, mean \pm SD = 1.02 ± 0.33 ml \cdot min $^{-1}$ \cdot g $^{-1}$, $n = 94$) as measured by PET. In each patient regions with reduced motility could be identified by radionuclide ventriculography. All patients had symptoms of ischemic heart disease and heart failure that were not fully controlled by medical therapy and prompted surgical referral. 10 patients were classified as NYHA class III and 5 as class II. 10 patients were on nitrates, 7 on β -blockers, 7 on calcium antagonists, 8 on ACE-inhibitors, and 5 on diuretics. No attempt was made to standardize medical therapy in these patients. A group of six normal male volunteers (aged 50 ± 2 years, range 46–56, $P = \text{NS}$ vs. patients) served as controls. All had a negative history for coronary heart disease, normal resting electrocardiograms, and negative exercise test in response to a high workload.

Radionuclide ventriculography. All subjects underwent radionuclide ventriculography (15) in order to assess regional wall motion and left ventricular ejection fraction.

Hyperinsulinemic euglycemic clamp. Patients were allowed a light breakfast only at least 4 h before this study. Prior to the PET scan (see below), a 20-G polyethylene cannula was inserted in a superficial forearm vein for infusion of glucose and insulin as described by DeFronzo et al. (16). A second cannula was threaded retrogradely into a superficial vein of the wrist or hand which had been arterialized using a heating pad set at 50°C. At time 0, a primed-constant insulin infusion (40 mU \cdot min $^{-1}$ per m 2 of body surface area) was started. The prime consisted of four times the final constant rate for the first 4 min, followed by two times the constant rate for 3 min. 4 min into the insulin infusion, an exogenous D-glucose infusion was started at an initial rate of 1.5 mg \cdot min $^{-1}$ per kg of body weight. Plasma glucose concentration in arterialized blood was measured at baseline and then every 5 min during the clamp. The glucose infusion rate was adjusted according to the change in plasma glucose during the preceding 5 min. Blood samples for insulin assay were taken from the arterialized vein at baseline (in all controls and nine patients) and 20, 40, and 60 min into the clamp (in all subjects). Under the near-steady state conditions of euglycemic hyperinsulinemia prevailing during the second hour of an insulin clamp, the exogenous glucose infusion rate equals the total amount of glucose metabolized by all tissues, and therefore is an index of whole-body insulin sensitivity (expressed in $\mu\text{mol} \cdot \text{min}^{-1}$ per kg of body weight).

Positron emission tomography. PET scanning was carried out in all subjects between 11 a.m. and 1 p.m. Scans were performed using an ECAT 931–08/12 scanner (CTI Inc., Knoxville, TN), which consists of eight rings of bismuth germanate crystal detectors. This scanner enables the acquisition of 15 planes of data over an axial field of view of 10.5 cm, thus allowing the whole heart to be imaged. The spatial resolution was of 8.4 mm full width at half maximum (FWHM) for the emission, and 7.7 mm FWHM for the transmission data at the center of the field of view, with a slice thickness of 6.6 mm FWHM (17). Subjects lay supine on the scanner bed. The optimal imaging position was determined using a 5-min rectilinear scan after exposure of the external ^{68}Ge ring source. A 20-min transmission scan was then performed in order to correct subsequent emission scans for tissue attenuation of the annihilation γ photons. After the transmission scan, the blood pool was imaged by inhalation of tracer amounts of ^{15}O -labeled carbon monoxide (C^{15}O), which labels erythrocytes through the formation of carboxyhemoglobin. C^{15}O was administered for 4 min at a concentration of 3 MBq/ml and a flow rate of 500 ml/min. A 6-min single-frame emission scan was initiated 1 min after the end of C^{15}O inhalation to allow for equilibration (18). Venous blood samples were taken every 1 min during the scan, and the C^{15}O concentration in whole blood was measured using a NaI well counter crosscalibrated with the scanner. After a 15-min period allowing for decay of ^{15}O radioactivity to background levels, myocardial blood flow (MBF) was measured using inhaled ^{15}O -labeled carbon dioxide (C^{15}O_2), which is rapidly converted to ^{15}O -labeled water (H_2^{15}O) by carbonic anhydrase in the lungs (18). C^{15}O_2 was inhaled for 3.5 min (4 MBq/ml

at a flow rate of 500 ml/min). A 25-frame dynamic PET scan covering a period of 7 min was started 30 s before C^{15}O_2 inhalation.

During the clamp, myocardial glucose utilization was measured with the glucose analogue FDG. FDG (185 MBq) was infused intravenously over 2 min using a pump, starting 30 s after the beginning of the scan. A 36-frame dynamic PET scan, with progressive increase in frame duration (1×30 s [background]; 12×10 s; 3×20 s; 4×30 s; 5×60 s; 4×150 s; 5×300 s; 2×600 s), was performed over a total period of 65 min. Arterialized whole blood was withdrawn continuously at a rate of 5 ml/min for the first 10 min and at a rate of 2.5 ml/min thereafter, and an on-line detection system, cross-calibrated against the PET scanner, was used to measure blood radioactivity (19). At set times (5, 10, 20, 45, and 60 min after FDG infusion) continuous blood withdrawal was interrupted briefly for the collection of blood samples which were used to calibrate the online blood curve and to determine plasma to whole blood radioactivity ratios. After each sample, the line was flushed with heparinized saline.

The study protocol was approved by the Research Ethics Committee of Hammersmith Hospital, and radiation exposure was licensed by the UK Administration of Radioactive Substances Advisory Committee (ARSAC). All patients gave informed and written consent before the study.

PET data analysis for cardiac measurements. All sinograms were corrected for tissue attenuation and reconstructed on a MicroVax II computer (Digital Equipment Corp., Marlboro, MA) using dedicated array processors and standard reconstruction algorithms. Images were transferred to SUN SPARC 2 workstations (Sun Microsystems, Mountain View, CA) for further analysis. Image manipulation and kinetic analyses were performed using the ANALYZE (Version 3.0; Biodynamics Research Unit, Mayo Foundation, Rochester, MN) and the MATLAB (The MathWorks Inc., Natick, MA) software packages, respectively. Cardiac images were resliced in the short axis view. Initially, myocardial blood volume (MBV) images were generated from the C^{15}O images as described previously (18). These images were used to position 2–4 regions of interest (ROI), each with an average size of 1.5 ml, in the left atrial chamber; thus, recovery of counts was greater than 90%. These ROIs were then projected onto the dynamic H_2^{15}O images in order to generate arterial time-activity curves. The average of these arterial curves was used as the arterial input function for the subsequent kinetic MBF analysis (18). In addition, these ROIs were projected onto the dynamic FDG study. However, to avoid spillover effects, the continuously monitored arterialized venous whole-blood curve was used to generate the input function for the kinetic FDG analysis. This curve was multiplied by the average plasma to whole-blood ratio, obtained from the discrete samples, in order to generate the plasma input function. A correction for the delay of this curve (arm and tubing) was made by shifting it so that the initial rise coincided with that from the atrial ROIs. Four equally spaced sectors corresponding to the anterior, septal, lateral, and inferior myocardium were defined separately on each plane of the last FDG frame. Within each sector three to four elliptical ROIs (1 ml each) were drawn. These ROIs were also projected onto the entire dynamic FDG and H_2^{15}O data sets, and tissue time-activity curves were generated for each ROI. The tissue H_2^{15}O time-activity curves were fitted for MBF and fraction of perfusable tissue (TF, the fraction of tissue within an ROI which exchanges water rapidly) using standard nonlinear regression techniques and a tracer kinetic model (18).

Tissue FDG time-activity curves were analysed by using the linearized approach proposed by Patlak et al. (20) for irreversible processes. The ratio of tissue to plasma concentration was plotted against the ratio of the integral of the plasma concentration to the plasma concentration, and a linear regression was performed for all data points corresponding to times greater than 10 min postinjection. The slope of this line provides the net influx rate of FDG. Myocardial glucose uptake (MGU) was then obtained by multiplying these regional influx rates by the plasma concentration of cold glucose, assuming a lumped constant of 1, and by dividing the product by the corresponding TF. This last step was performed in order to correct for partial

volume effects. A conversion for milliliters to grams of perfusable tissue was made by dividing the flow and metabolic data by the tissue density (1.04 g/ml). Thus, MGU is expressed as $\mu\text{mol}\cdot\text{min}^{-1}$ per g of perfusable tissue.

PET data analysis for skeletal muscle measurements. This was similar to that used for the heart except that a different image zoom factor was used in the reconstruction. In addition, images were not resliced. The ROI was traced on the medial skeletal muscles of both arms, but the results reported are only relative to the arm contralateral to the FDG injection site (usually the left). For both H_2^{15}O and FDG the same input functions were used as for the myocardial analyses. The skeletal muscle H_2^{15}O time-activity curves were fitted for blood flow and the distribution volume of water as described previously (21). The FDG analysis was identical to that used for the myocardium, except that no final normalization to tissue fraction could be applied.

Arm skeletal muscle data (glucose uptake [SGU] and blood flow [SBF]) were available for only 12 of the 15 patients because of a loss of computer data. Since at steady state tissue uptake equals the product of blood flow by the arterio-venous (A-V) concentration gradient, the ratio of PET-derived MGU (or skeletal muscle glucose uptake [SGU]) to MBF (or SBF) is equal to the A-V glucose gradient across cardiac (or skeletal) muscle.

Statistical analysis. All the data are presented as mean \pm SEM. Mann-Whitney U test was used to compare mean group values, whereas paired comparisons were performed by Wilcoxon signed-rank test. Regression analysis was performed according to standard techniques. A value of $P < 0.05$ was considered statistically significant.

Results

Patient characteristics. The body mass index (wt/ht^2) was 24 ± 1 kg/m^2 in controls and 25 ± 1 kg/m^2 in patients ($P = \text{NS}$). Baseline plasma glucose concentrations (measured before the clamp) were 5.2 ± 0.4 mM in controls and 6.1 ± 0.2 mM in patients ($P = \text{NS}$). Global left ventricular ejection fraction was $59\pm 5\%$ in controls and $38\pm 3\%$ in patients ($P = 0.01$).

Physiological measurements during clamp. During the study, the rate-pressure product was 6079 ± 579 mmHg·bpm in controls and 5773 ± 479 in patients ($P = \text{NS}$). Plasma glucose was clamped at 6.0 ± 0.4 mM in controls and at 5.6 ± 0.2 mM in patients ($P = \text{NS}$). Fasting plasma insulin levels were 49 ± 14 and 144 ± 45 pmol/liter in controls and patients, respectively ($P < 0.05$). During the clamp, steady-state plasma insulin concentrations were 474 ± 36 and 516 ± 36 pmol/liter in controls and patients, respectively ($P = \text{NS}$). The glucose metabolized by the whole body during the last 60 min of the clamp was 37 ± 4 $\mu\text{mol}\cdot\text{min}^{-1}\cdot\text{kg}^{-1}$ in controls and 14 ± 2 $\mu\text{mol}\cdot\text{min}^{-1}\cdot\text{kg}^{-1}$ in patients ($P = 0.001$).

Cardiac and skeletal FDG uptake and blood flow. (Table I). The rate of glucose uptake in myocardial regions showing normal contraction on radionuclide ventriculography and nor-

mal blood flow (> 0.69 $\text{ml}\cdot\text{min}^{-1}\cdot\text{g}^{-1}$) averaged 0.38 ± 0.03 $\mu\text{mol}\cdot\text{min}^{-1}\cdot\text{g}^{-1}$ in patients, a 46% reduction as compared to the mean value of controls (0.70 ± 0.03 $\mu\text{mol}\cdot\text{min}^{-1}\cdot\text{g}^{-1}$). Tissue fraction in these myocardial regions was similar in patients and controls (0.77 ± 0.03 vs. 0.76 ± 0.04 g/ml, $P = \text{NS}$). Skeletal muscle glucose uptake was 0.056 ± 0.015 $\mu\text{mol}\cdot\text{min}^{-1}\cdot\text{g}^{-1}$ in control subjects and 0.026 ± 0.015 $\mu\text{mol}\cdot\text{min}^{-1}\cdot\text{g}^{-1}$ in patients, a 54% reduction. In contrast, there was no difference between the two groups in myocardial or skeletal muscle blood flow rates.

On the pooled data from all study subjects, both cardiac ($r = 0.76$, $P < 0.001$) and skeletal muscle ($r = 0.82$, $P < 0.001$), glucose uptake were linearly related to whole-body glucose utilization (Fig. 1). Furthermore, myocardial and SGU were directly related to one another ($r = 0.78$, $P < 0.0001$) (Fig. 2). A significant positive relationship was also found between myocardial and skeletal muscle blood flow ($r = 0.65$, $P < 0.01$), whereas there was no relation of either with whole-body glucose uptake. In the patient group, there was no correlation between the ejection fraction and cardiac ($r = 0.03$, $P = 0.9$), skeletal muscle ($r = 0.32$, $P = 0.3$) or whole-body glucose utilization ($r = 0.11$, $P = 0.7$). Furthermore, there was no significant difference in cardiac, skeletal muscle, or whole-body glucose uptake between groups of patients with different medical therapy.

Discussion

PET is the only nuclear medicine technique that can theoretically give an absolute quantification of metabolic processes. In the case of FDG measurements, however, there are some assumptions that must be discussed. The affinities of FDG for glucose transporters and hexokinase are not always identical with those of glucose. To account for this difference, the estimate of glucose uptake obtained from FDG-PET is normally divided by the so-called lumped constant. The value of the lumped constant has been measured in the hearts of rabbits (22–24) and dogs (25), and had been found to be constant over a range of insulin and glucose concentrations as well as during anoxia. However, other authors have reported variability of the lumped constant in perfused rat hearts with the addition of insulin (26, 27), and have recommended that PET studies of FDG uptake in the heart should be performed under controlled metabolic conditions. For this reason, the studies here reported have been performed during steady-state conditions of hyperinsulinemia and euglycemia as realized by the insulin clamp technique. The mathematical model we used for the analysis of FDG-PET data, the Patlak model (20), also assumes that FDG-6-phosphate dephosphorylation is negligible.

Table I. Myocardial and Skeletal Muscle Blood Flow and Glucose Uptake Rates during Euglycemic Hyperinsulinemia

	Controls	Patients	P
Myocardial blood flow ($\text{ml}\cdot\text{min}^{-1}\cdot\text{g}^{-1}$)	1.09 ± 0.06	0.97 ± 0.14	NS
Myocardial glucose uptake ($\mu\text{mol}\cdot\text{min}^{-1}\cdot\text{g}^{-1}$)	0.70 ± 0.03	0.38 ± 0.03	$P = 0.0005$
Myocardial A-V glucose gradient (mM)	0.65 ± 0.04	0.41 ± 0.04	$P = 0.002$
Muscle blood flow ($\text{ml}\cdot\text{min}^{-1}\cdot\text{g}^{-1}$)	0.046 ± 0.012	0.043 ± 0.006	NS
Muscle glucose uptake ($\mu\text{mol}\cdot\text{min}^{-1}\cdot\text{g}^{-1}$)	0.056 ± 0.006	0.026 ± 0.004	$P = 0.005$
Muscle A-V glucose gradient (mM)	1.35 ± 0.29	0.75 ± 0.15	$P = 0.08$

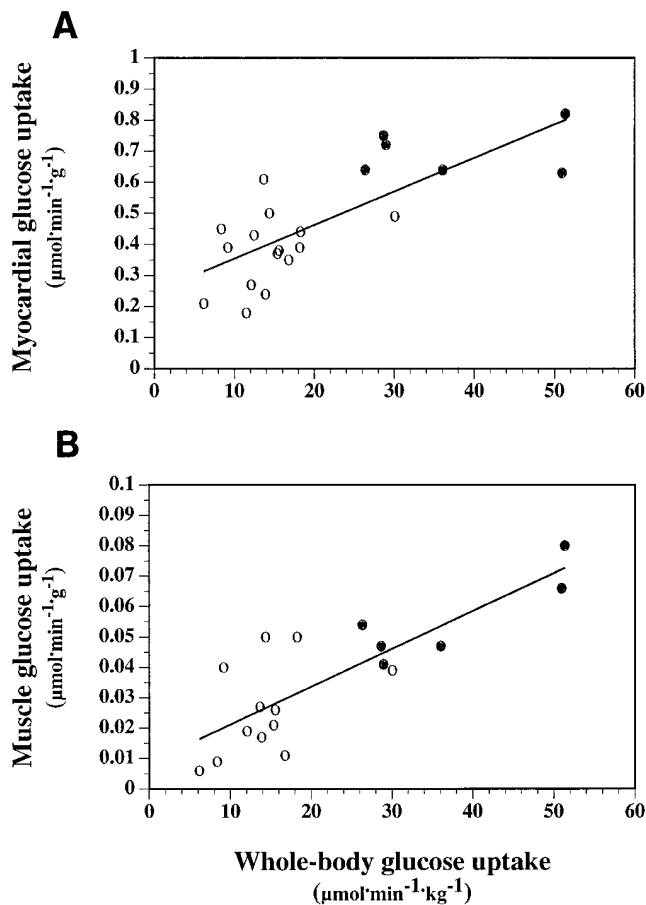


Figure 1. Relationship between myocardial glucose uptake (A) and SGU (B) and whole-body glucose utilization. Healthy controls are indicated by the gray circles, the patients by the empty circles.

This has been verified by various studies during PET (22, 24, 28, 29). However, the values of the lumped constant and the rate of FDG-6-phosphate dephosphorylation are not known in man, and this remains a limitation of the technique (14).

Despite the assumptions inherent in the method, the current PET results agree very well with measurements obtained using different techniques. Thus, the arm skeletal muscle blood flow rates measured by PET in the present study are in the range of those measured in the forearm of healthy subjects during a euglycemic clamp with the use of an indicator dilution method (30) or by venous occlusion plethysmography (31). Likewise, our PET estimates of myocardial and skeletal muscle glucose gradients are very similar to those measured during simultaneous arterial and coronary sinus catheterization (5) and the perfused forearm technique (32), respectively, at insulin doses identical to those used in the present study. Finally, from the current PET data on arm SGU—and assuming that in adults skeletal muscle is 40% of body weight (33)—it can be calculated that whole-body skeletal muscle represented $70\pm 9\%$ of whole-body glucose utilization, a figure in full accord with previous estimates (34–36). There were additional findings of physiological interest. Thus, though myocardial glucose uptake was 8 ± 2 times larger than SGU per unit of tissue mass, myocardial blood flow was 18 ± 3 times higher than skeletal muscle blood flow. Consequently, the skeletal muscle A-V

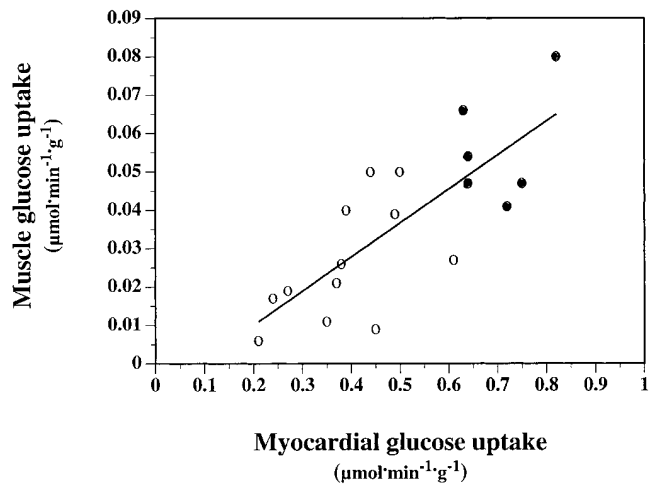


Figure 2. Relationship between myocardial and skeletal muscle glucose uptake. Healthy controls are indicated by the gray circles, the patients by the empty circles.

glucose gradient was 80% larger than the corresponding A-V gradient across the heart ($P < 0.002$). This finding indicates that, even at rest striated muscle is more sensitive to insulin than myocardial tissue, which achieves higher rates of glucose utilization by virtue of a higher perfusion rate. Moreover, myocardial and skeletal muscle blood flow, despite being largely different in absolute terms, were directly related to one another, and bore no relation to whole-body or regional insulin sensitivity. Overall, the picture emerging from these PET measurements is internally consistent and physiologically compatible.

The main finding of the present study is that patients with a history of myocardial infarction present insulin resistance at the whole body level as well as in skeletal muscle and myocardial muscle as compared to healthy subjects of similar age and body mass. Of particular significance is the fact that insulin resistance was detected in noninfarcted, normally contractile myocardium, which presumably had undergone compensatory hypertrophy. To rule out the possibility that admixture of scar tissue with preserved myocardium might have artificially lowered insulin-stimulated uptake, only segments with normal wall motion and blood flow were selected. Furthermore, tissue fraction (the fraction of tissue volume in rapid exchange with water, which has been shown to be reduced in scarred myocardium [37]) was comparable in noninfarcted areas of patients and normal myocardium of controls. In the patients, myocardial glucose uptake was reduced in the face of normal blood flow rates, clearly indicating a cellular impairment in glucose extraction. Finally, the degree of insulin resistance in the heart was coherent with that simultaneously measured in skeletal muscle and at the whole-body level (Figs. 1 and 2). Taken together, these findings are compatible with a state of generalized, flow-independent insulin resistance. This situation contrasts with that of IDDM, in which skeletal muscle is resistant but cardiac muscle is not (10, 11), and that of NIDDM, in which the reverse combination has been reported (12).

Some epidemiological studies have shown an association of ischemic heart disease with raised fasting plasma insulin concentrations, an index of insulin resistance, but others have not

(38). In general, the association has been weak, and more convincingly shown for lipid abnormalities than for coronary artery disease itself (39–42). However, a recent prospective study has documented a significantly higher risk for ischemic heart disease in hyperinsulinemic Canadian men independently of serum triglycerides, cholesterol fractions, and apolipoprotein B (43). Case-control investigations have consistently shown that patients with coronary heart disease are insulin resistant at the whole body level when compared to subjects free of ischemic heart disease on equal grounds of confounding factors (i.e., sex, age, body weight, glucose tolerance, blood pressure, and serum lipid levels) (41, 44, 45). Our study is in line with these results, and provides direct evidence that even the well perfused, normally contracting myocardial regions are resistant to insulin, in a similar degree to skeletal muscle.

In severe heart failure, Swan et al. (8) have reported the presence of insulin resistance, and have subsequently shown that the degree of resistance is not related to the etiology (ischemic heart disease vs. dilated cardiomyopathy) but rather to the severity of heart failure (46). In the patients in the present study, who had variable degrees of cardiac insufficiency, SGU under the influence of insulin was markedly reduced. This is another manifestation of a metabolic abnormality of skeletal muscle in heart failure, similar to what has been shown for oxidative phosphorylation rates by ^{31}P nuclear magnetic resonance (47). The question arises, whether the cardiac insulin resistance of our patients was entirely secondary to heart failure. Indeed, in a patient population with less severe coronary artery disease and no signs of heart failure, Baliga et al. also showed peripheral but not cardiac insulin resistance (48). How much of the decrease in cardiac FDG uptake depends on alterations specific to heart muscle and how much could be a response to a generalized metabolic abnormality remains to be assessed. The first hypothesis is supported by the finding of decreased levels of GLUT-4 mRNA in an animal model of cardiac hypertrophy (49). However, this observation needs to be confirmed in patients. The second hypothesis is suggested by the fact that circulating free fatty acids are increased in heart failure (50), possibly as a consequence of the increased norepinephrine concentrations seen in heart failure (51). Norepinephrine can increase free fatty acid (FFA) levels (52), and FFA in turn can decrease glucose utilization both in heart (5) and skeletal muscle (53) by substrate competition (54). Because norepinephrine levels would be expected to be higher in the patients with the largest reduction in ejection fraction, cardiac insulin resistance should be proportional to the ejection fraction. In our data, we could not find any correlation between ejection fraction and insulin sensitivity. Nevertheless, it remains possible that both mechanisms (reduced cellular response to insulin and enhanced substrate competition) contribute to cardiac and skeletal muscle insulin resistance in these patients.

Although all our study subjects were sedentary, patients with compromised cardiovascular status would be expected to exercise less than matched controls. Because physical exercise affects insulin sensitivity (55), reduced physical fitness could contribute to the skeletal muscle insulin resistance of our patients. While this remains a potential mechanism, it may be observed that exercise results in enhanced glucose uptake and blood flow in response to insulin mostly in the muscle groups that perform work (56, 57). In contrast, we did not find any change in resting skeletal (arm) blood flow in our patient

group. While there is increasing evidence in favor of a decreased skeletal muscle blood flow during exercise in heart failure (58), the results reported at rest are conflicting (59–62). This may be due to differences in the severity of cardiac dysfunction in the patient populations examined by different authors as well as to the techniques used.

Our results are relevant to the long debated question of the efficacy of glucose-insulin-potassium therapy in myocardial infarction (63, 64). A recent study (65) has shown that the infusion of glucose and insulin after a myocardial infarction improves the long-term prognosis of diabetic patients. Thus, insulin resistance per se is not a contraindication to metabolic therapy, and might be a target for therapeutic intervention.

References

1. Reaven, G.M. 1988. Role of insulin resistance in human disease. *Diabetes*. 37:1595–607.
2. Opie, L.H. 1991. *The Heart, Physiology and Metabolism*. Raven Press, New York.
3. Coleman, G.M., S. Gradinac, H. Taegtmeier, M. Sweeney, and O.H. Frazer. 1989. Efficacy of metabolic support with glucose-insulin-potassium for left ventricular pump failure after aortocoronary bypass surgery. *Circulation*. 80:191–196.
4. Oliver, M.F., and L.H. Opie. 1994. Effects of glucose and fatty acids on myocardial ischaemia and arrhythmias. *Lancet*. 343:155–158.
5. Ferrannini, E., D. Santoro, R. Bonadonna, A. Natali, O. Parodi, and P.G. Camici. 1993. Metabolic and hemodynamic effects of insulin on human hearts. *Am. J. Physiol.* 264:E308–E315.
6. Rogers, W.J., R.O. Russell, Jr., H.G. McDaniel, and C.E. Rackley. 1977. Acute effects of glucose-insulin-potassium infusion on myocardial substrates, coronary blood flow and oxygen consumption in man. *Am. J. Cardiol.* 40:421–428.
7. Scheuer, J. 1993. Metabolic factors in myocardial failure. *Circulation*. 87:VII54–VII57.
8. Swan, J.W., C. Walton, I.F. Godsland, A.L. Clark, A.J. Coats, and M.F. Oliver. 1994. Insulin resistance in chronic heart failure. *Eur. Heart J.* 15:1528–1532.
9. Sun, D., N. Nguyen, T.R. DeGrado, M. Schwaiger, and F.C.R. Brosius. 1984. Ischemia induces translocation of the insulin-responsive glucose transporter GLUT4 to the plasma membrane of cardiac myocytes. *Circulation*. 89:793–798.
10. Nuutila, P., J. Knuuti, U. Ruotsalainen, V.A. Koivisto, E. Eronen, M. Teras, J. Bergman, M. Haaparanta, L. Voipio-Pulkki, and J. Viikari, et al. 1993. Insulin resistance is localized to skeletal but not heart muscle in type 1 diabetes. *Am. J. Physiol.* 264:E756–762.
11. vom Dahl, J., W.H. Herman, R.J. Hicks, F.J. Ortiz Alonso, K.S. Lee, K.C. Allman, E.R. Wolfe, Jr., V. Kalff, and M. Schwaiger. 1993. Myocardial glucose uptake in patients with insulin-dependent diabetes mellitus assessed quantitatively by dynamic positron emission tomography. *Circulation*. 88:395–404.
12. Voipio Pulkki, L.M., P. Nuutila, M.J. Knuuti, U. Ruotsalainen, M. Haaparanta, M. Teras, U. Wegelius, and V.A. Koivisto. 1993. Heart and skeletal muscle glucose disposal in type 2 diabetic patients as determined by positron emission tomography. *J. Nucl. Med.* 34:2064–2067.
13. Nuutila, P., M. Maki, H. Laine, M.J. Knuuti, U. Ruotsalainen, M. Luotolahti, M. Haaparanta, O. Solin, A. Jula, V.A. Koivisto, et al. 1995. Insulin action on heart and skeletal muscle glucose uptake in essential hypertension. *J. Clin. Invest.* 96:1003–1009.
14. Hicks, R.J., W.H. Herman, V. Kalff, E. Molina, E.R. Wolfe, G. Hutchins, and M. Schwaiger. 1991. Quantitative evaluation of regional substrate metabolism in the human heart by positron emission tomography. *J. Am. Coll. Cardiol.* 18:101–111.
15. Zaret, B.L., F.J. Wackers. 1993. Nuclear cardiology (2). *N. Engl. J. Med.* 329:855–863.
16. DeFronzo, R.A., J.D. Tobin, and R. Andres. 1979. Glucose clamp technique: a method for quantifying insulin secretion and resistance. *Am. J. Physiol.* 237:E214–E223.
17. Spinks, T.J., T. Jones, M.C. Gilardi, and J.D. Heather. 1988. Physical performance of the latest generation of commercial positron scanner. *IEEE Trans. Nucl. Med.* NS-35:721–725.
18. Araujo, L.I., A.A. Lammertsma, C.G. Rhodes, E.O. McFalls, H. Iida, E. Rechavia, A. Galassi, R. De Silva, T. Jones, and A. Maseri. 1991. Noninvasive quantification of regional myocardial blood flow in coronary artery disease with oxygen-15-labeled carbon dioxide inhalation and positron emission tomography. *Circulation*. 83:875–885.
19. Lammertsma, A.A., C.J. Bench, G.W. Price, J.E. Cremer, S.K. Luthra,

- D. Turton, N.D. Wood, and R.S. Frackowiak. 1991. Measurement of cerebral monoamine oxidase B activity using L-[¹¹C]deprenyl and dynamic positron emission tomography. *J. Cereb. Blood Flow Metab.* 11:545–556.
20. Patlak, C.S., R.G. Blasberg, and J.D. Fenstermacher. 1983. Graphical evaluation of blood-to-brain transfer constants from multiple-time uptake data. *J. Cereb. Blood Flow Metab.* 3:1–7.
21. Wilson, C.B.J.H., A.A. Lammerstma, C.G. McKenzie, K. Sikora, and T. Jones. 1992. Measurements of blood flow and exchanging water space in breast tumors using positron emission tomography: a rapid and non-invasive dynamic method. *Cancer Res.* 52:1592–1597.
22. Huang, S.C., B.A. Williams, J.R. Barrio, J. Krivokapich, C. Nissenson, E.J. Hoffman, and M.E. Phelps. 1987. Measurement of glucose and 2-deoxy-2-[¹⁸F]fluoro-D-glucose transport and phosphorylation rates in myocardium using dual-tracer kinetic experiments. *FEBS Lett.* 216:128–132.
23. Krivokapich, J., S.C. Huang, C.E. Selin, and M.E. Phelps. 1987. Fluoro-deoxyglucose rate constants, and glucose metabolic rate in rabbit heart. *Am. J. Physiol.* 252:H777–787.
24. Marshall, R.C., S.C. Huang, W.W. Nash, and M.E. Phelps. 1983. Assessment of the [¹⁸F]fluoro-deoxyglucose kinetic model in calculations of myocardial glucose metabolism during ischemia. *J. Nucl. Med.* 24:1060–1064.
25. Ratib, O., M.E. Phelps, S.C. Huang, E. Henze, C.E. Selin, and H.R. Schelbert. 1982. Positron tomography with deoxyglucose for estimating local myocardial glucose metabolism. *J. Nucl. Med.* 23:577–586.
26. Hariharan, R., M. Bray, R. Ganim, T. Doenst, G.W. Goodwin, and H. Taegtmeyer. 1995. Fundamental limitations of [¹⁸F]2-deoxy-2-fluoro-D-glucose for assessing myocardial glucose uptake. *Circulation.* 91:2435–2444.
27. Russell, R.R., J.M. Mrus, J.I. Mommessin, and H. Taegtmeyer. 1992. Compartmentation of hexokinase in rat heart. A critical factor for tracer kinetic analysis of myocardial glucose metabolism. *J. Clin. Invest.* 90:1972–1977.
28. Gambhir, S.S., M. Schwaiger, S.C. Huang, J. Krivokapich, H.R. Schelbert, C.A. Nienaherr, and M.E. Phelps. 1989. Simple noninvasive quantification method for measuring myocardial glucose utilization in humans employing positron emission tomography and fluorine-18 deoxyglucose. *J. Nucl. Med.* 30:359–366.
29. Nguyen, V.T., K.A. Mossberg, T.J. Tewson, W.H. Wong, R.W. Rowe, G.M. Coleman, and H. Taegtmeyer. 1990. Temporal analysis of myocardial glucose metabolism by 2-[¹⁸F]fluoro-2-deoxy-D-glucose. *Am. J. Physiol.* 259:H1022–H1031.
30. Bonadonna, R.C., M.P. Saccomani, L. Seely, K.S. Zych, E. Ferrannini, C. Cobelli, and R.A. DeFronzo. 1993. Glucose transport in human skeletal muscle. The in vivo response to insulin. *Diabetes.* 42:191–198.
31. Kelley, D.E., and L.J. Mandarino. 1990. Hyperglycemia normalizes insulin-stimulated skeletal muscle glucose oxidation and storage in non-insulin-dependent diabetes mellitus. *J. Clin. Invest.* 86:1999–2007.
32. Ebeling, P., R. Bourey, L. Koranyi, J.A. Tuominen, L.C. Groop, J. Henriksson, M. Mueckler, A. Sovijärvi, and V.A. Koivisto. 1993. Mechanism of enhanced insulin sensitivity in athletes. *J. Clin. Invest.* 92:1623–1631.
33. Natali, A., G. Buzzigoli, S. Taddei, D. Santoro, M. Cerri, R. Pedrinelli, and E. Ferrannini. 1990. Effects of insulin on hemodynamics and metabolism in human forearm. *Diabetes.* 39:490–500.
34. DeFronzo, R.A., E. Jacot, E. Jequier, E. Maeder, J. Wahren, and J.P. Felber. 1981. The effect of insulin on the disposal of intravenous glucose. Results from indirect calorimetry and hepatic and femoral venous catheterization. *Diabetes.* 30:1000–1007.
35. Yki-Järvinen, H., A.A. Young, C. Lamkin, and J.E. Foley. 1987. Kinetics of glucose disposal in whole body and across the forearm in man. *J. Clin. Invest.* 79:1713–1719.
36. Mitrakou, A., D.E. Kelley, T. Veneman, T. Jenssen, T. Pangburn, J. Reilly, and J. Gerich. 1990. Contribution of abnormal muscle and liver glucose metabolism to postprandial hyperglycemia in NIDDM. *Diabetes.* 39:1381–1390.
37. Iida, H., C.G. Rhodes, R. de Silva, Y. Yamamoto, L.I. Araujo, A. Maseri, and T. Jones. 1991. Myocardial tissue fraction-correction for partial volume effects and measure of tissue viability. *J. Nucl. Med.* 32:2169–2175.
38. Wingard, D.L., and E. Barrett-Connor. 1995. Heart disease and diabetes. In *Diabetes in America*, 2nd ed. NIH Publication No. 95-1468, Bethesda, MD. 429–448.
39. Fontbonne, A. 1994. Why can high insulin levels indicate a risk for coronary heart disease? *Diabetologia.* 37:953–955.
40. Jarrett, R.J. 1994. Why is insulin not a risk for coronary heart disease? *Diabetologia.* 37:945–947.
41. Reaven, G.M., and A. Laws. 1994. Insulin resistance, compensatory hyperinsulinemia, and coronary heart disease. *Diabetologia.* 37:948–952.
42. Stern, M.P. 1994. The insulin resistance syndrome: the controversy is dead, long live the controversy! *Diabetologia.* 37:956–958.
43. Despres, J.-P., B. Lamarche, P. Mauriège, B. Cantin, G.R. Dagenais, S. Moorjani, and P.-J. Lupien. 1996. Hyperinsulinemia as an independent risk factor for ischemic heart disease. *N. Engl. J. Med.* 334:952–957.
44. Paolisso, G., A. Gambardella, D. Galzerano, A. D'Amore, V. Balbi, M. Varricchio, and F. D'Onofrio. 1993. Metabolic features of patients with and without coronary heart disease but with superimposable cluster of cardiovascular risk factors. *Coron. Artery. Dis.* 4:1085–1091.
45. Bressler, P., S.R. Bailey, M. Matsuda, and R.A. DeFronzo. Insulin resistance and coronary heart disease. *Diabetologia.* In press.
46. Swan, J.W., C. Walton, I.F. Godsland, and A.L. Clark. 1994. Relationship of insulin resistance to the severity and etiology of chronic heart failure. *Circulation.* 90:1–174.
47. Massie, B., M. Conway, R. Yonge, S. Frostick, P. Sleight, et al. 1987. ³¹P nuclear magnetic resonance evidence of abnormal skeletal muscle metabolism in patients with congestive heart failure. *Am. J. Cardiol.* 60:309–315.
48. Baliga, R., A. Lammertsma, C. Rhodes, T. Aitman, J. Scott, and J.S. Kooner. 1995. Positron emission tomography localises insulin resistance to skeletal muscle in premature coronary disease. *Circulation.* 92:1–16.
49. Paternostro, G., K. Clarke, J. Health, A.M. Seymour, and J.K. Radda. 1995. Decreased GLUT-4 mRNA content and insulin-sensitive deoxyglucose uptake show insulin resistance in the hypertensive rat heart. *Cardiovasc. Res.* 30:205–211.
50. Paolisso, G., A. Gambardella, D. Galzerano, A. D'Amore, P. Rubino, M. Verza, P. Teasuro, M. Varricchio, and F. D'Onofrio. 1994. Total-body and myocardial substrate oxidation in congestive heart failure. *Metab. Clin. Exp.* 43:174–179.
51. Thomas, J.A., and B.H. Marks. 1978. Plasma norepinephrine in congestive heart failure. *Am. J. Cardiol.* 41:233–243.
52. Marangou, A.G., F.P. Alford, G. Ward, F. Liskaser, P.M. Aitken, K.M. Weber, R.C. Boston, and J.D. Best. 1988. Hormonal effects of norepinephrine on acute glucose disposal in humans: a minimal model analysis. *Metab. Clin. Exp.* 37:885–891.
53. Nuutila, P., V.A. Koivisto, J. Knuuti, U. Ruotsalainen, M. Teras, et al., 1992. Glucose-free fatty acid cycle operates in human heart and skeletal muscle in vivo. *J. Clin. Invest.* 89:1767–1774.
54. Randle, P.J., P.B. Garland, C.N. Hales, and E.A. Newsholme. 1963. The glucose fatty-acid cycle: its role in insulin sensitivity and metabolic disturbances of diabetes mellitus. *Lancet.* 1:785–789.
55. Devlin, J.T. 1992. Effects of exercise on insulin sensitivity in humans. *Diabetes Care.* 15(Suppl. 4):1690–1693.
56. Annuzzi, G., G. Riccardi, B. Capaldo, and L. Kaijser. 1991. Increased insulin-stimulated glucose uptake by exercised human muscle one day after prolonged physical exercise. *Eur. J. Clin. Invest.* 21:6–12.
57. Hardin, D.S., B. Azzarelli, J. Edwards, J. Wigglesworth, L. Maianu, G. Brechtel, A. Johnson, A. Baron, and W.T. Garvey. 1995. Mechanisms of enhanced insulin sensitivity in endurance-trained athletes: effects on blood flow and differential expression of GLUT4 in skeletal muscles. *J. Clin. Endocrinol. Metab.* 80:2437–2446.
58. Sullivan, M.J., and M.H. Hawthorne. 1995. Exercise intolerance in patients with chronic heart failure. *Prog. Cardiovasc. Dis.* 38:1–22.
59. Massie, B., M. Conway, R. Yonge, S. Frostick, J. Ledingham, et al., 1987. Skeletal muscle metabolism in patients with congestive heart failure: relation to clinical severity and blood flow. *Circulation.* 76:1009–1019.
60. Reading, J.L., J.M. Goodman, M.J. Plyley, J.S. Floras, P.P. Liu, et al., 1993. Vascular conductance and aerobic power in sedentary and active subjects and heart failure patients. *J. Appl. Physiol.* 74:567–573.
61. Wilson, J.R., J.L. Martin, D. Schwartz, and N. Ferraro. 1984. Exercise intolerance in patients with chronic heart failure: role of impaired nutritive flow to skeletal muscle. *Circulation.* 69:1079–1087.
62. Zelis, R., S.H. Nellis, J. Longhurst, G. Lee, and D.T. Mason. 1975. Abnormalities in the regional circulations accompanying congestive heart failure. *Prog. Cardiovasc. Dis.* 18:181–199.
63. Opie, L.H. 1995. Glucose and the metabolism of ischaemic myocardium. *Lancet.* 345:1520–1521.
64. Taegtmeyer, H. 1995. Is there a rationale for glucose-insulin-potassium therapy in acute myocardial infarction? *Cardiol. Rev.* 3:307–313.
65. Malmberg, K., and L. Ryden. 1994. Insulin-glucose infusion in diabetic patients with acute myocardial infarction reduces longterm mortality. *Circulation.* 90:1–168.